Journal of Neuroscience Research 00:000–000 (2007)

# Glucose and Hippocampal Neuronal Excitability: Role of ATP-Sensitive Potassium Channels

**Chin-Wei Huang,[1,2] Chao-Ching Huang,[2,3] Juei-Tang Cheng,[4] Jing-Jane Tsai,[1] and Sheng-Nan Wu[5]★**

[1]Department of Neurology, National Cheng Kung University Medical Center, Tainan, Taiwan
[2]Institute of Clinical Medicine, National Cheng Kung University Medical Center, Tainan, Taiwan
[3]Department of Pediatrics, National Cheng Kung University Medical Center, Tainan, Taiwan
[4]Department of Pharmacology, National Cheng Kung University Medical Center, Tainan, Taiwan
[5]Department of Physiology, National Cheng Kung University Medical Center, Tainan, Taiwan

Hyperglycemia-related neuronal excitability and epileptic seizures are not uncommon in clinical practice. However, their underlying mechanism remains elusive. ATP-sensitive $K^+$ ($K_{ATP}$) channels are found in many excitable cells, including cardiac myocytes, pancreatic β cells, and neurons. These channels provide a link between the electrical activity of cell membranes and cellular metabolism. We investigated the effects of higher extracellular glucose on hippocampal $K_{ATP}$ channel activities and neuronal excitability. The cell-attached patch-clamp configuration on cultured hippocampal cells and a novel multielectrode recording system on hippocampal slices were employed. In addition, a simulation modeling hippocampal CA3 pyramidal neurons (Pinsky-Rinzel model) was analyzed to investigate the role of $K_{ATP}$ channels in the firing of simulated action potentials. We found that incremental extracellular glucose could attenuate the activities of hippocampal $K_{ATP}$ channels. The effect was concentration dependent and involved mainly in open probabilities, not single-channel conductance. Additionally, higher levels of extracellular glucose could enhance neuropropagation; this could be attenuated by diazoxide, a $K_{ATP}$ channel agonist. In simulations, high levels of intracellular ATP, used to mimic increased extracellular glucose or reduced conductance of $K_{ATP}$ channels, enhanced the firing of action potentials in model neurons. The stochastic increases in intracellular ATP levels also demonstrated an irregular and clustered neuronal firing pattern. This phenomenon of $K_{ATP}$ channel attenuation could be one of the underlying mechanisms of glucose-related neuronal hyperexcitability and propagation. 

**Key words:** glucose; hippocampus; ATP-sensitive potassium channel; excitability

Glucose plays a major role in metabolism and cerebral functions. However, the effects of hyperglycemia on the central nervous system (CNS) and neuronal excitability (Biessels et al., 1994; Stewart and Liolista, 1999; Gispen and Biessels, 2000) are not fully understood. Hyperglycemia-related seizures, not uncommon in clinical practice (Singh et al., 1973; Singh and Strobos, 1980; Venna and Sabin, 1981), deserve special attention insofar as they can cause significant damage. Experimentally, the correlation between extracellular glucose concentration and excitability (seizure) has been established in previous studies (Margineanu et al., 1998; Tutka et al., 1998; Schwechter et al., 2003). Although vascular compromise has been considered important in altered synaptic plasticity (Kamal et al., 2006), the specific mechanisms on neuronal excitability remain largely elusive.

ATP-sensitive $K^+$ ($K_{ATP}$) channels exist in many excitable cells, including cardiac myocytes, pancreatic β cells, muscle cells, and neurons (Liu et al., 1999, Seino, 1999). In pancreatic β cells, these channels are known to couple cellular metabolism to electrical activity by opening and closing as the intracellular ATP/ADP ratio decreases and increases, respectively (Ashcroft and Gribble, 1998). They are octameric complexes composed of four pore-forming units with inward rectifying characteristics (Kir 6.1 or Kir 6.2) and four sulfonylurea (SUR) binding sites (SUR1 or SUR2), regulated by intracellular ATP as well as pharmacological agents (e.g., diazoxide).

In pancreatic β cells, elevation in blood glucose and the closure of $K_{ATP}$ channels trigger events leading to calcium influx, cellular depolarization, and insulin secretion

Contract grant sponsor: National Science Council; Contract grant number: NSC-94-2314-B-006-040; Contract grant number: NSC-94-2320-B-006-019; Contract grant number: NSC-95-2314-B-006-046; Contract grant sponsor: National Cheng Kung University Medical Center, Taiwan; Contract grant number: NCKUH-2006-029.

★Correspondence to: Sheng-Nan Wu, MD, PhD, Department of Physiology, National Cheng-Kung University Medical Center, No. 1 University Road, Tainan City 70101, Taiwan. E-mail: snwu@mail.ncku.edu.tw

Received 29 September 2006; Revised 16 January 2007; Accepted 18 January 2007

**Published online 00 Month 2007 in Wiley InterScience (www.interscience.wiley.com). DOI: 10.1002/jnr.21284**

(Miki and Seino, 2005). In the CNS, $K_{ATP}$ channels exist in many tissues, particularly the hippocampus and neocortex (Dunn-Meynell et al., 1998). Except for a similar role in sensing central glucose in hypothalamic glucose-responsive neurons (Miki et al., 2001), they are not involved in specific neuroendocrine functions. Therefore, a second, more general role for these channels, functionally expressed in neurons, has be investigated. Owing to the abundant expression of $K_{ATP}$ in the brain (Hicks et al., 1994; Mourre et al., 1990), the activation of $K_{ATP}$ channels during ATP-depleted conditions has become a subject of studies. Mice lacking Kir6.2 (Kir 6.2−/− mice) are vulnerable to hypoxia, exhibiting a reduced threshold for generalized seizure (Yamada et al., 2001). Transgenic mice, overexpressing the SUR1 gene in the forebrain, show a significant increase in the threshold for kainate-induced seizures (Hernandez-Sanchez et al., 2001). However, with excessive extracellular glucose and ATP in the hippocampal neurons, how $K_{ATP}$ channels react is still marginally understood.

Therefore, here we investigate the effects of increased extracellular glucose on $K_{ATP}$ channel activity in hippocampal neurons. We provide the first direct evidence that increases in extracellular glucose and intracellular ATP attenuate $K_{ATP}$ channels, with cells becoming more depolarized, leading to a more excitable state.

## MATERIALS AND METHODS

### Cell Preparation

Our H19-7 cell line, originally derived from hippocampi dissected from day 17 embryonic (E17) Holtzman rat embryos and preserved by retroviral transduction of temperature-sensitive tsA58 SV40 large T antigen, was obtained from the American Type Culture Collection (Manassas, VA; CRL-2526; Morrione et al., 2000). It had hippocampal neuron characteristics (Morrione et al., 2000; Bhargava et al., 2002; Huang et al., 2004, 2005). H19-7 cells were maintained in Dulbecco's modified Eagle's media with 4 mM L-glutamine, adjusted to contain 1.5 g/liter $NaHCO_3$ and 4.5 g/liter glucose supplemented with 10% fetal bovine serum, 200 μg/ml G418, and 1 μg/ml puromycin, in flasks coated with 15 μg/ml poly-L-lysine. They were equilibrated in humidified 5% $CO_2$/95% $O_2$ at air temperature, 34°C. Experiments were performed after 5 days of subcultivation (60–80% confluence) with cells from passages 2 and 4.

### Cell Differentiation

For differentiation experiments, H19-7 cells were plated at a $10^5$ cells/35-mm plate density in medium containing serum at a permissive temperature (34°C). After 18 hr, the cells were washed extensively and shifted to a nonpermissive temperature (39°C) in N2 SFM (DMEM-high glucose medium supplemented with 0.11 mg/ml sodium pyruvate, 2 mM glutamine, 0.1 mg/ml transferrin, 20 nM progesterone, 0.1 mM putrescine, and 30 nM sodium selenite) supplemented with 50 ng/ml insulin-like growth factor-I (IGF-I; Life Technologies). After 48 hr, the cells in which neurite formation was seen were harvested and analyzed for electrophysiological experiments (Kim et al., 1997; Morrione et al., 2000). Rat hippocampal neuron-derived H19-7 cells could proliferate at the permissive temperature in response to IGF or differentiate to a neuronal phenotype in N2 medium at the nonpermissive (Eves et al., 1992; Morrione et al., 2000).

### Electrophysiological Measurements

Immediately before each experiment, cells were dissociated with an aliquot of cell suspension transferred to a recording chamber positioned on the stage of an inverted microscope (DM IL; Leica Microsystems, Wetzlar, Germany). The microscope was coupled to a video camera system, with magnification up to ×1,500, to monitor cell size continuously during the experiments. Cells were bathed at room temperature (20–25°C) in normal Tyrode's solution containing 1.8 mM $CaCl_2$. The recording pipettes were pulled from thin-walled borosilicate glass capillaries (Kimax-51; Kimble Glass, Vineland, NJ) using a two-stage microelectrode puller (PP-830; Narishige, Tokyo, Japan), and the tips were fire-polished with a microforge (MF-83; Narishige). When filled with pipette solution, their resistance ranged between 3 and 5 MΩ.

Ion currents were recorded with glass pipettes in a patch-clamp cell-attached configuration, using an RK-400 patch-clamp amplifier (Bio-Logic, Claix, France; Wu et al., 2000a,b). All potentials were corrected for liquid junction potential. Tested drugs were perfused or added to the bath to obtain the final concentration indicated.

### Preparation of Rat Hippocampal Slices

All experiments were performed in accordance with the specifications of the Ethical Committee of National Cheng-Kung University. Male Sprague-Dawley rats, 2–3 weeks old, were used for all experiments. They were housed under constant temperature (22°C ± 2°C) with a 12-hr light cycle, then decapitated after halothane anesthesia. Transverse slices of hippocampus (350 μm thick) were prepared with a vibrating tissue slicer (DTK-1000; Dosaka, Japan). This was performed in artificial cerebrospinal fluid (ACSF) composed of (mM) NaCl 124, KCl 3, $NaHCO_3$ 26, $CaCl_2$ 2, $MgSO_4$ 1, $KH_2PO_4$ 1.25, and d-glucose 10, saturated with 95%$O_2$/5%$CO_2$ at pH 7.4 at 4°C. Slices were transferred to an ACSF holding chamber for equilibration at room temperature. Electrophysiological recordings were made at least 1 hr after recovery of the slices.

### Preparation of Multielectrode Dish Recording System

The 64-channel multielectrode dish (MED64) system (Alpha MED Sciences, Tokyo, Japan), a novel two-dimensional neuronal electroactivity monitoring technique based on methods described by Oka et al. (1999) and Shimono et al. (2000), was employed in this study. We used MED-P530A probes (Alpha MED Sciences) with 300 μM interpolar distance of electrodes, chamber depth at 10 mm, and 64 planar microelectrodes in an 8 × 8 array for determination of propagation patterns in hippocampal evoked field potentials, including presynaptic fiber volley (PrV), an indicator of presynaptic intraneuronal response, and field excitatory postsynaptic potentials (fEPSP), an indicator of postsynaptic α-amino-3-

hydroxy-5-methyl-4-isoxazolepropionic acid (AMPA)/glutamate receptor response.

During electrophysiological recordings, an individual hippocampal slice was positioned on the MED64 probe on a fine mesh net and with adequate anchorage. The probe was composed of transparent liquid crystal materials, except for the electrodes, allowing electrode localization in the slice under a microscope. The probe was superfused with control glucose-free ACSF at 32°C (2 ml/min flow rate). A single planar microelectrode with bipolar constant current pulses (60 μA, 0.1 msec) was used for stimulation. Stimulation patterns were designed in data acquisition software (Panasonic MED conductor) and delivered through the isolator (BSI-2: Alpha MED Sciences). These procedures of electroevoked stimulation were controlled by a computer running under Windows NT. When the signal-to-noise (S/N ratio) was above 3, detectable responses were recorded. Responses in all electrodes were evaluated and compared in a centrifugal fashion from the stimulating electrode.

Visually detectable and undetectable signal changes in the central electrodes and the peripheral electrodes, respectively, were designated *responder* and *nonresponder*, respectively. Propagation area and amplitude of PrV and fEPSP were recorded with all 64 microelectrodes (Okada et al., 2003; Huang et al., 2006b). 6,7-Dinitroquinoxaline-2,3-dione (DNQX, an AMPA/glutamate receptor inhibitor) was dissolved in dimethyl sulfoxide (DMSO) before addition to the bath. EPSPs were verified by the addition of DNQX. Bicuculline (10 μM), a $GABA_A$ antagonist, was added to enhance field potentials. For paired pulse facilitation, two fEPSPs were evoked with twin pulses at 60-msec interpulse intervals. Ratios of the second to the first potential were determined.

## Data Recording and Analysis

Signals consisting of voltage and current tracings were displayed on an analog/digital oscilloscope (HM 507; Hameg Inc., East Meadow, NY). Data were stored online through a high-speed/low-noise analog/digital interface (Digidata 1322A; Axon Instruments, Union City, CA) controlled by a commercially available software package (pCLAMP 9.0; Axon Instruments). The sampling rate for electrophysiological measurements was 10 kHz. Current was low-pass filtered at 1 or 3 kHz. Ion currents recorded during experiments were stored and subsequently analyzed in pCLAMP 9.0 (Axon Instruments), Origin 7.5 (Microcal Software, Inc., Northampton, MA), SigmaPlot 7.0 (SPSS, Inc., Apex, NC), or custom Excel macros (Microsoft, Redmond, WA). The pCLAMP-generated voltage-step protocols were often used to examine the current-voltage (I-V) relations for ionic currents.

Single-channel currents from $K_{ATP}$ channels were analyzed in pCLAMP 9.0. Multigaussian adjustments of the amplitude distributions between channels were used to determine unitary currents. Functional independence between channels was verified by comparing the observed stationary probabilities with values calculated according to binomial law. Active channel number in patch N was counted at the end of each experiment and used to normalize the opening probability at each potential. Opening probabilities were evaluated by using an iterative process to minimize the $\chi^2$ calculated with sufficient independent observations. The number of channels per patch was determined at the level of −100 mV in inside-out patches bathed in an ATP-free concentration.

Channel activity, recorded from a patch, was expressed as $N \cdot P_o$, which can be estimated using the following equation: $N \cdot P_o = (A_1 + 2A_2 + 3A_3 + \ldots + nA_n)/(A_0 + A_1 + A_2 + A_3 + \ldots + A_n)$, where N is the number of active channels in the patch, $A_0$ is the area under the curve of an all-points histogram corresponding to the closed state, and $A_1 \ldots A_n$ represent the histogram areas reflecting the levels of distinct open states for 1 to n channels in the patch. The bin number performed for amplitude histogram was 0.2 pA for each interval. The level of zero-current event was determined based on Gaussian distribution obtained at the level of closed state in the channel.

Mean results are presented as mean values ± SEM. Paired or unpaired *t*-tests and one-way ANOVA with the least significance difference method for multiple comparisons were used for statistical evaluation of differences among mean values. Significance was set at $P < 0.05$.

Field data recorded during MED64 experiments were analyzed in various software programs (PanasonicMED Conductor), including Origin 7.5 and custom Excel macros. Data were expressed as mean ± SEM. Total amplitudes of PrV and fEPSP responses were analyzed by repeated ANOVA measurements. Differences between values were considered significant at $P < 0.05$.

## Drugs and Solutions

All chemicals, including diazoxide, nicorandil, carbonyl cyanide m-cholorophenylhydrazone (CCCP), DNQX, and bicuculline, were obtained from Sigma (St. Louis, MO) and were of reagent grade. The composition of normal Tyrode's solution was 136.5 mM NaCl, 5.4 mM KCl, 1.8 mM $CaCl_2$, 0.53 mM $MgCl_2$, 5.5 mM glucose, and 5.5 mM HEPES-NaOH buffer, pH 7.4. To record $K^+$ currents, the patch pipette was filled with a solution consisting of 140 mM KCl, 1 mM $MgCl_2$, 3 mM $Na_2ATP$, 0.1 mM $Na_2GTP$, 0.1 mM EGTA, and 5 mM HEPES-KOH buffer, pH 7.2. In most single-channel recordings, high-$K^+$ bathing solution contained 145 mM KCl, 0.53 mM $MgCl_2$, and 5 mM HEPES-KOH, pH 7.4, and the pipette solution contained 145 mM KCl, 2 mM $MgCl_2$, and 5 mM HEPES-KOH, pH 7.2. To attain osmolarity control, NaCl concentration in the Tyrode's solution was adjusted to maintain osmolarity of 280–290 mOsm.

## Mathematical Modeling

High expression of $K_{ATP}$ channels in CA3 neurons (seizure-prone area) has been discussed in several papers (Griesemer et al., 2002; Quinta-Ferreira and Matias, 2005). In addition, the important role of CA3 neurons in kindling temporal lobe seizures has also been established (Treherne and Ashford, 1991; Jang et al., 2006). Spontaneous discharge of neurons was mathematically reconstructed using the model of hippocampal CA3 pyramidal neurons originally derived from Pinsky and Rinzel (1994). The formulation, which reproduces the behavior of CA3 pyramidal neurons, consists of a fast and

**TABLE I. Default Parameters Used for Modeling Hippocampal CA3 Pyramidal Neurons**

| Symbol | Description | Value |
|---|---|---|
| Cm | Membrane capacitance | 3 μF |
| $g_{Na}$ | $Na^+$ current conductance | 18 pS |
| $g_{Kdr}$ | Delayed rectifier $K^+$ current conductance | 15 pS |
| $g_{Ca}$ | $Ca^{2+}$ current conductance | 1 nS |
| $g_{Kahp}$ | After hyperpolarization $K^+$ current | 0.8 nS |
| $g_{KCa}$ | $Ca^{2+}$ activated $K^+$ conductance | 20 nS |
| $g_{Katp}$ | ATP-sensitive $K^+$ current conductance | 0.3 nS |
| $V_{Ca}$ | $Ca^{2+}$ reversal potential | +80 mV |
| $V_{Na}$ | $Na^+$ reversal potential | +60 mV |
| $V_K$ | $K^+$ reversal potential | −75 mV |

transient $Na^+$ current; a persistent, depolarization-activated $Na^+$ current; a low-threshold $Ca^{2+}$ current; a high-threshold $Ca^{2+}$ current; a $Ca^{2+}$-activated $K^+$ current; a transient outward $K^+$ current; a slowly inactivating $K^+$ current; a hyperpolarization-activated cation current; and an ATP-sensitive $K^+$ current. Because of the extent to which formulations of ion currents and model predictions have been validated, this model has been applied for simulation studies. The source file for this model is readily available at http://cams.njit.edu/~vbooth/. The solutions to the different sets of ordinary differential equations in the simulations were approximated in the X-Win32 version of XPPAUT on a Dell Precision 670 workstation (Ermentrout, 2002; Wu and Chang, 2006). The information for XPP software is available at http://www.math.pitt.edu/~bard/XPP/XPP.html. XPPAUT uses concise, straightforward code, making it easy to translate to other languages and packages. The conductance values and reversal potentials, together with parameters used to solve the set of differential equations, are listed in Table I. T1

To incorporate stochastic dynamics into the differential equations from the model, $I_{K(ATP)}$ was rewritten as $I_{K(ATP)} = g_{KATP\text{-}max} \times s \times (V - E_K)$, where $s$ satisfies the stochastic differential equation (Higham, 2001):

$$ds = [\alpha(1 - s) - \beta s]dt + \sigma dw \text{ and}$$

$$\sigma = [\alpha(1 - s) + \beta s]/[(\tau N_{K(ATP)}]^{1/2}.$$

In these simulations, noise in resting membrane potential was generated by Gaussian random variations arising from the concentrations of intracellular ATP. In the deterministic limit, $s$ approaches its mean value, $s_0 = \alpha/(\alpha + \beta)$.

Both deterministic and stochastic stimulations were performed using the stochastic Euler algorithm as implemented in the program XPP (Ermentrout, 2002). Briefly,

$$s_{n+1} = s_n + [\alpha(1 - s_n) - \beta s_n]\Delta t + \sigma_n \Delta w_n,$$

where $\Delta w_n$ is a Gaussian random variable with mean 0 and variance $\Delta t$.

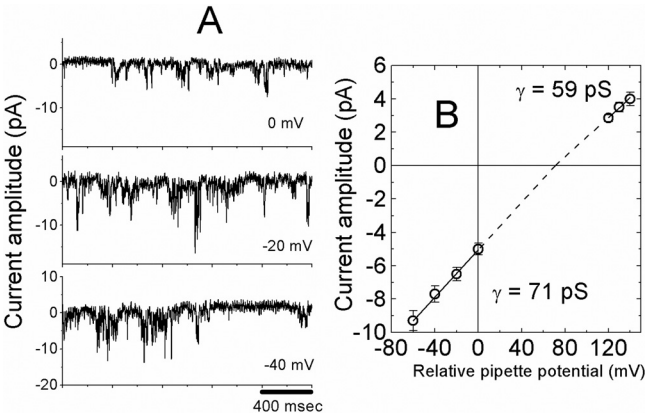


Fig. 1. **A:** Current tracings of single channel recordings measured in differentiated H19-7 cells. $K_{ATP}$ channel activity at various membrane potentials was examined, and the plot of current amplitude, as a function of holding potential, was then constructed. **B:** Averaged current-voltage relation of single $K_{ATP}$ channel currents in differentiated H19-7 cells. The single-channel conductance of these channels, calculated from a linear current-voltage relationship, was 71 ± 1.5 pS (n = 8) at hyperpolarized potentials with a reversal potential of 68 ± 2 mV (n = 8). Of note was that the inward conductance evoked by hyperpolarization (71 pS) from the reversal potential is greater than in response to depolarizations (59 pS).

## RESULTS

### Characterization of $K_{ATP}$ Channels in Differentiated H19-7 Cells

Figure 1A shows the current tracings of single-channel recordings. The cells were bathed in $Ca^{2+}$-free Tyrode's solution with the holding potentials at 0, −20, and −40 mV. After patch excision, $K_{ATP}$ channel currents occurred in rapid open-close transitions and in brief bursts with a unitary current amplitude near 4.0 ± 1.1, 6.3 ± 1.0, and 7.8 ± 1.3 pA (n = 7) at the levels of 0, −20, and −40 mV, respectively. $K_{ATP}$ channel activity at various pipette potentials was examined and the plot of current amplitude, as a function of holding potential, constructed. F1

Figure 1B illustrates the averaged current-voltage relation of $K_{ATP}$ single channel currents in differentiated H19-7 cells. The single-channel conductance of these channels, calculated from a linear current-voltage relationship, was 71 ± 1.5 pS (n = 8) at hyperpolarized potentials with a reversal potential of 68 ± 2 mV (n = 8). The inward conductance evoked by hyperpolarization (71 pS), extrapolated from the reversal potential, was greater than that elicited by depolarization (59 pS). Results are in line with the characteristics of minor inward rectification in $K_{ATP}$ channels.

### Effects of Glucose on $K_{ATP}$ Channels in Differentiated H19-7 Cells

Glucose effects on $K_{ATP}$-channel activity were examined. In Figure 2A, under symmetrical $K^+$ (145 mM) conditions, $K_{ATP}$ channel activity was observed at F2

J_ID: Z3P Customer A_ID: 21284 Cadmus Art: JNR21284 Date: 22-MARCH-07 Stage: I Page: 5



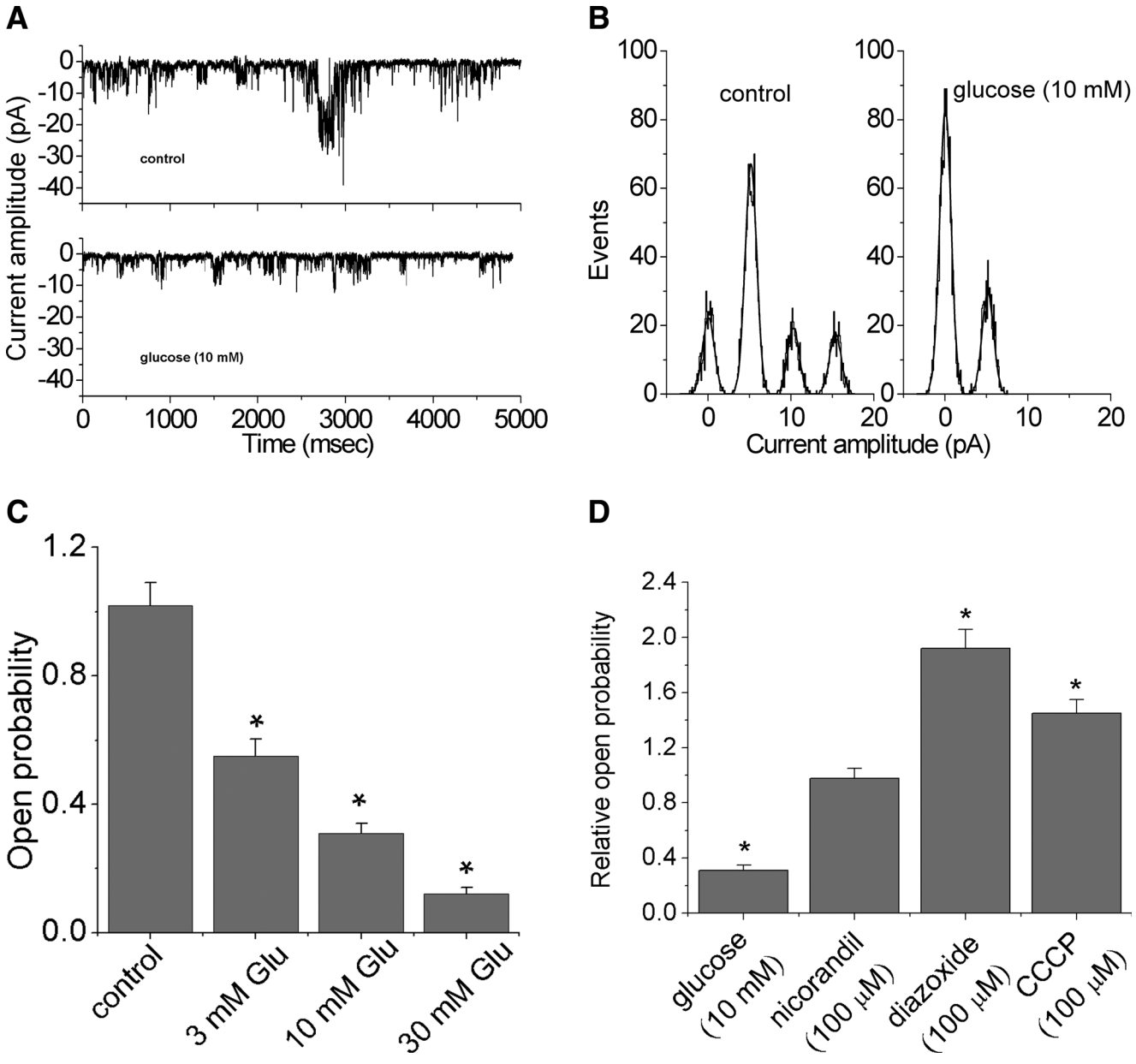


Fig. 2. **A:** Glucose effect on $K_{ATP}$ channel activity attenuation in differentiated H19-7 cells. When glucose (10 mM) was added to the bath, channel activity was significantly attenuated. **B:** There was no significant difference in the amplitude of unitary inward current between the absence and the presence of 10 mM glucose (5.1 ± 0.7 pA vs. 5.1 ± 0.8 pA; n = 7). All points shown in the amplitude histograms were fitted by one or more Gaussian distributions using maximum likelihood. **C:** A concentration-dependent glucose-induced attenuation of $K_{ATP}$ channel activity. *Significantly different from control ($P < 0.05$). Each point represents the mean ± SEM (n = 5–8). **D:** Further $K_{ATP}$ channel activity characterization in differentiated H19-7 cells. Effects of nicorandil, diazoxide, and CCCP, in the absence of glucose, were examined. Addition of glucose (10 mM) produced an inhibitory effect on channel activity. *Significantly different ($P < 0.05$).

−60 mV in cell-attached configuration; the control solution was glucose-free. Interestingly, when glucose (10 mM) was added to the bath, channel activity was significantly attenuated. $K_{ATP}$ channels had rapid open-close transitions and brief bursts. However, there was no discernible difference in unitary inward current amplitude between the absence and the presence of 10 mM glucose (5.1 ± 0.7 pA vs. 5.1 ± 0.8 pA; n = 7; Fig. 2B).

## Concentration-Dependent Effect of Glucose on $K_{ATP}$ Channel Activities

The relationship between the concentration of glucose and the open probability of $K_{ATP}$ channels, in differentiated H19-7 cells, was further investigated. This series of experiments was conducted with symmetrical $K^+$ concentrations (145 mM). The cell-attached configuration was used with a holding potential of −60 mV. Figure 2C



ID: kumarpr Date: 22/3/07 Time: 16:46 Path: J:/Production/JNR#/Vol00000/070091/3B2/C2JNR#070091

J_ID: Z3P Customer A_ID: 21284 Cadmus Art: JNR21284 Date: 22-MARCH-07 Stage: I Page: 6



demonstrates a concentration-dependent, glucose-induced attenuation of $K_{ATP}$ channel activity. There were significant differences in $K_{ATP}$ channel activity between the cells exposed to 3, 10, and 30 mM of glucose and the control group (n = 5–8 in each group).

### Comparisons With Various Agents on the Effects on $K_{ATP}$ Channel Activity

For further characterization of $K_{ATP}$ channel activity in differentiated H19-7 cells, the effects of nicorandil, diazoxide, and CCCP, known $K_{ATP}$ channel activity manipulators, were examined. Cells were bathed in symmetrical $K^+$ (145 mM) solution with a −60-mV holding potential. $K_{ATP}$ channel activity, without glucose, was considered 1.0; activities with glucose (10 mM) or other compounds were compared and plotted. As shown in Figure 2D, the relative open probabilities after nicorandil (100 μM), diazoxide (100 μM), and CCCP (100 μM) addition in the control solution were 1.05 ± 0.05 (n = 5), 1.9 ± 0.1 (n = 5), and 1.5 ± 0.07 (n = 6), respectively; the probability was 0.3 ± 0.05 (n = 6) with 10 mM glucose. $K_{ATP}$ channel agonists (nicorandil, diazoxide) are known to exert an opening effect. In our study, diazoxide, but not nicorandil, significantly increased $K_{ATP}$ channel activity in these cells. As an uncoupler, CCCP led to metabolic inhibition and reduced intracellular ATP levels, producing a relative $K_{ATP}$ channel activity increase in these cells. Our results clearly characterize the properties of $K_{ATP}$ channels in differentiated H19-7 cells.

### Effects of Glucose on Field Potential Properties in Hippocampal Slices

For further delineation of glucose and $K_{ATP}$ channel activity effects on neuronal excitability and propagation, we used a novel multielectrode recording system (MED64). Relative electrode positions on the hippocampal slice are shown in Figure 3A. As demonstrated in Figure 3B,C, in the presence of a $GABA_A$ antagonist (10 μM bicuculline), glucose addition (20 mM) exerted no significant effect on presynaptic fiber volleys or the paradigm of paired-pulse facilitation. However, during exposure to 20 mM glucose, an increase in fEPSP amplitude was noted (n = 8).

F3

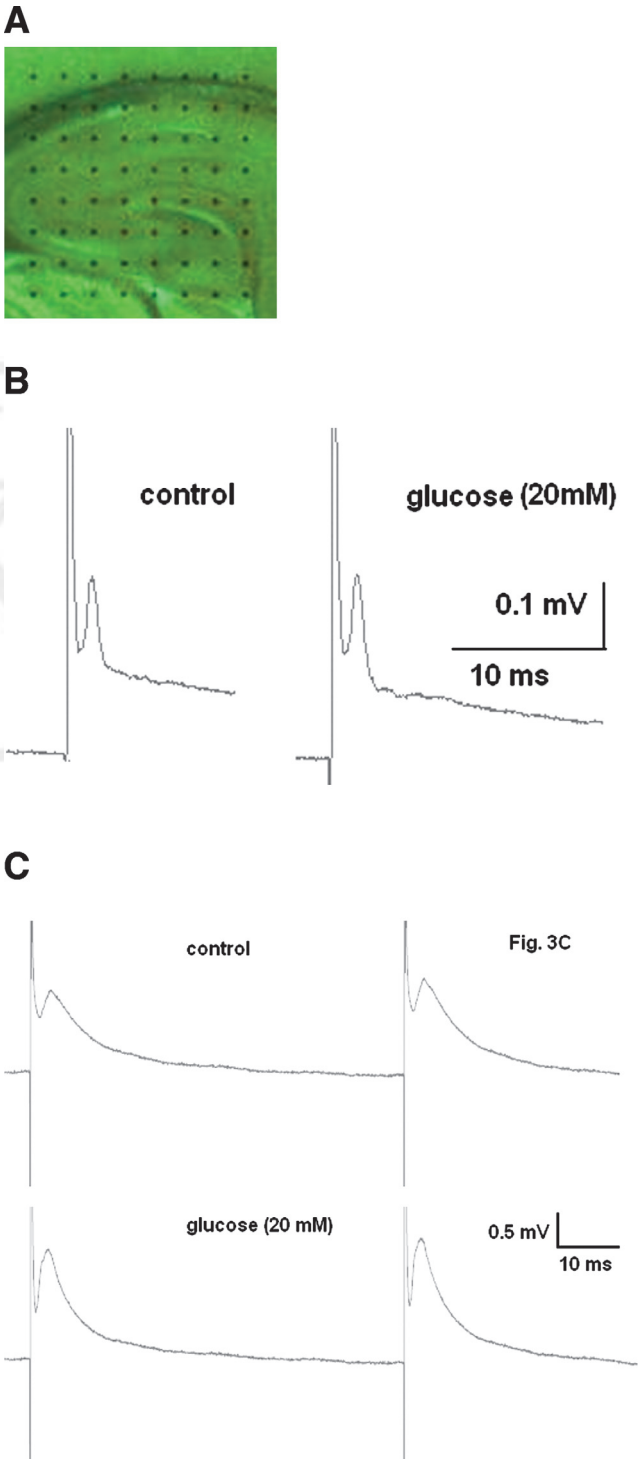


Fig. 3. Further delineation of the effects of glucose and $K_{ATP}$ channel activity on neuronal excitability and propagation, by the multielectrode recording system (MED64). **A:** Representative photograph of the relative positions of the multielectrodes on the hippocampal slice. In the presence of the $GABA_A$ antagonist bicuculline (10 μM), addition of glucose (20 mM) exerted no significant effect on presynaptic fiber volleys (control: 0.13 ± 0.02 mV vs. glucose: 0.128 ± 0.01 mV). **B:** The paradigm of paired-pulse facilitation. The ratio of paired-pulse facilitation was 1.32 ± 0.07 before and 1.22 ± 0.06 after the addition of glucose (**C**). However, an enhancing effect on fEPSP amplitude was noted (C; n = 8).

### Effects of Glucose and $K_{ATP}$ Channel Opener Diazoxide on Neuropropagation

Enhancement of fEPSP, in both propagation and amplitude, were demonstrated and evaluated in experiments on hippocampal slices. Figure 4A shows the representative selected sites for control, and Figure 4B shows the same sites with enhanced fEPSP after addition of

F4

COLOR



ID: kumarpr Date: 22/3/07 Time: 16:46 Path: J:/Production/JNR#/Vol00000/070091/3B2/C2JNR#070091

J_ID: Z3P Customer A_ID: 21284 Cadmus Art: JNR21284 Date: 22-MARCH-07 Stage: I Page: 7



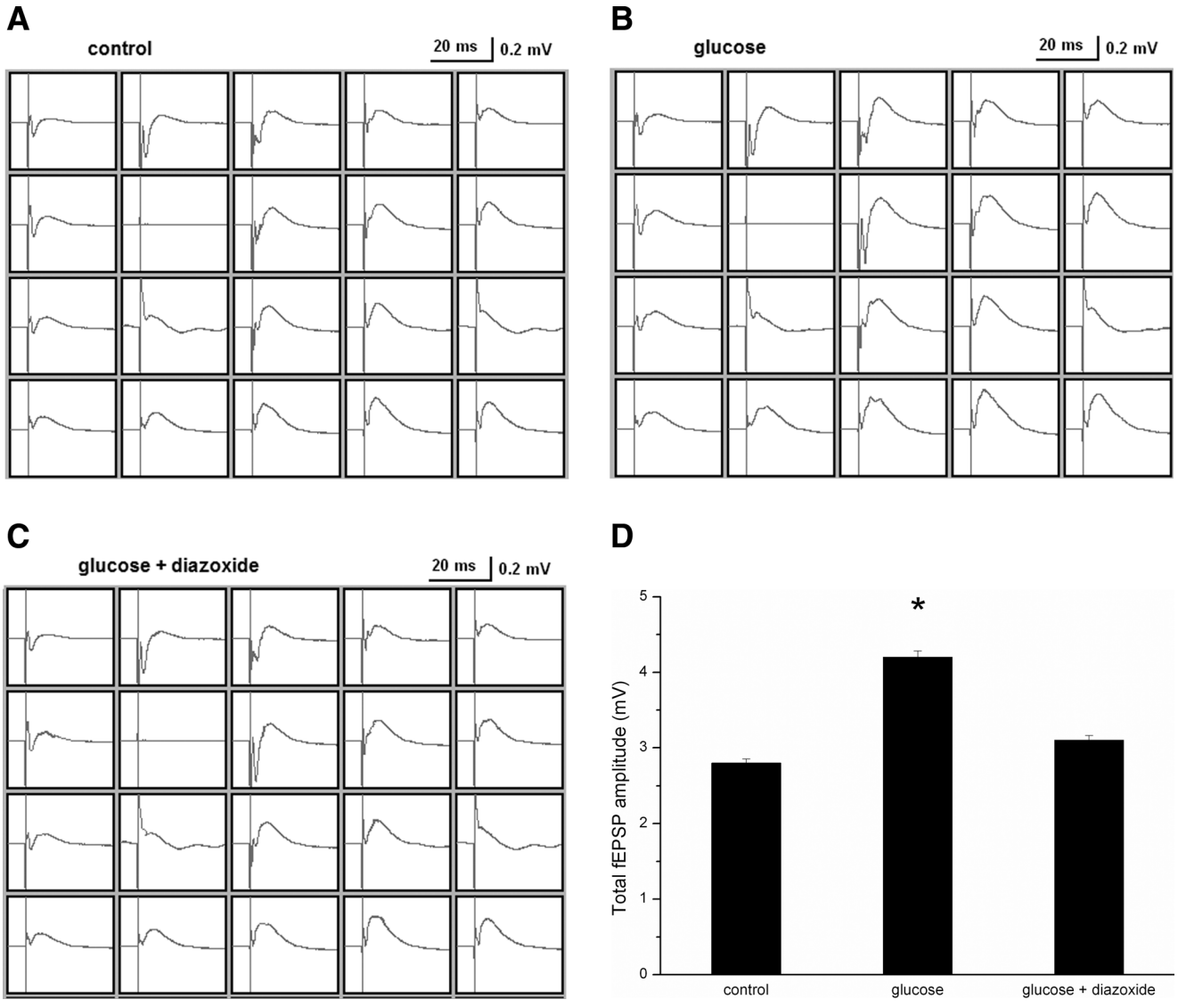


Fig. 4. Evoked fEPSP in MED64 recording. Representative figures (selected sites only) of control solution (**A**) and the addition of glucose (20 mM; **B**) exerting an enhancing effect, both on the propagation and on the amplitude of fEPSP. **C:** Addition of diazoxide attenuated the enhanced effect by glucose. **D:** The total fEPSP amplitudes in control, with addition of glucose, and with addition of diazoxide were 2.8 ± 0.5, 4.3 ± 0.9, and 3.1 ± 0.7 mV, respectively (n = 8). *Significantly different from control ($P < 0.05$).

20 mM glucose; Figure 4C shows that the enhancement was attenuated by addition of the $K_{ATP}$ channel opener diazoxide, in both fEPSP amplitude and propagation (n = 8). Total fEPSP amplitudes were 2.8 ± 0.5, 4.3 ± 0.9, and 3.1 ± 0.7 mV, respectively (Fig. 4D).

### Glucose and Pregabalin Effects on $K_{ATP}$ Channel Acitivty in Simulated Hippocampal CA3 Pyramidal Neurons

To determine how $K_{ATP}$ channel activity alters the discharge pattern of hippocampal neurons and to address questions difficult to study experimentally, a simulator was used. Derived from Pinsky and Rinzel (1994), it is based primarily on the electrophysiological properties of hippocampal CA3 pyramidal neurons. In this modeled neuron, when extracellular glucose is increased from 5.5 to 30 mM (concentration of intracellular ATP increased from 0.1 to 0.3 mM), action potential firing increased (Fig. 5A), together with a reduction in $K_{ATP}$ channel conductance (Fig. 5B). F5

There was an inverse relationship between $K_{ATP}$ channel current peak amplitude and firing frequency (Fig. 5C). To mimic intracellular physiological conditions, we used a stochastic simulation to study intracellular ATP level effects on action potential firing. As can be seen in Figure 6A, when mean intracellular ATP concentration was increased to 0.1 mM, in addition to mild depolarization, the increased firing rate demonstrated irregularity. F6



ID: kumarpr Date: 22/3/07 Time: 16:47 Path: J:/Production/JNR#/Vol00000/070091/3B2/C2JNR#070091

J_ID: Z3P Customer A_ID: 21284 Cadmus Art: JNR21284 Date: 22-MARCH-07 Stage: I Page: 8



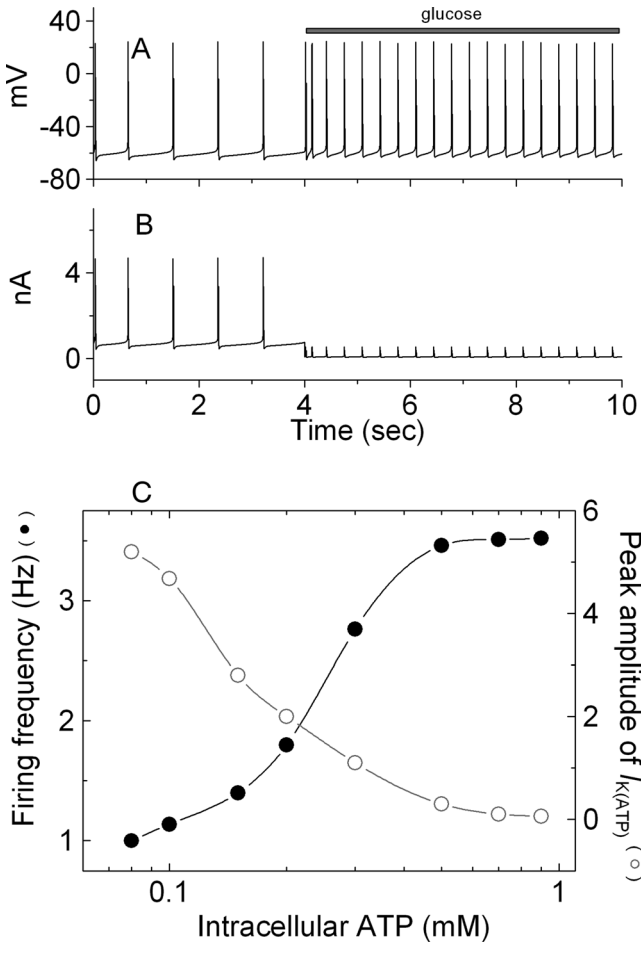


Fig. 5. Simulation model, based on the electrophysiological properties of hippocampal CA3 pyramidal neurons. When extracellular glucose was increased from 5.5 to 30 mM, the membrane depolarized with increased firing of action potentials (**A**), together with reduced conductance of $K_{ATP}$ channels, as shown in **B**. **C:** Action potential firing frequency increased, corresponding to the concentration of intracellular ATP. The peak amplitude of $K_{ATP}$ current demonstrated an inverse relationship with firing frequency and increment of ATP.

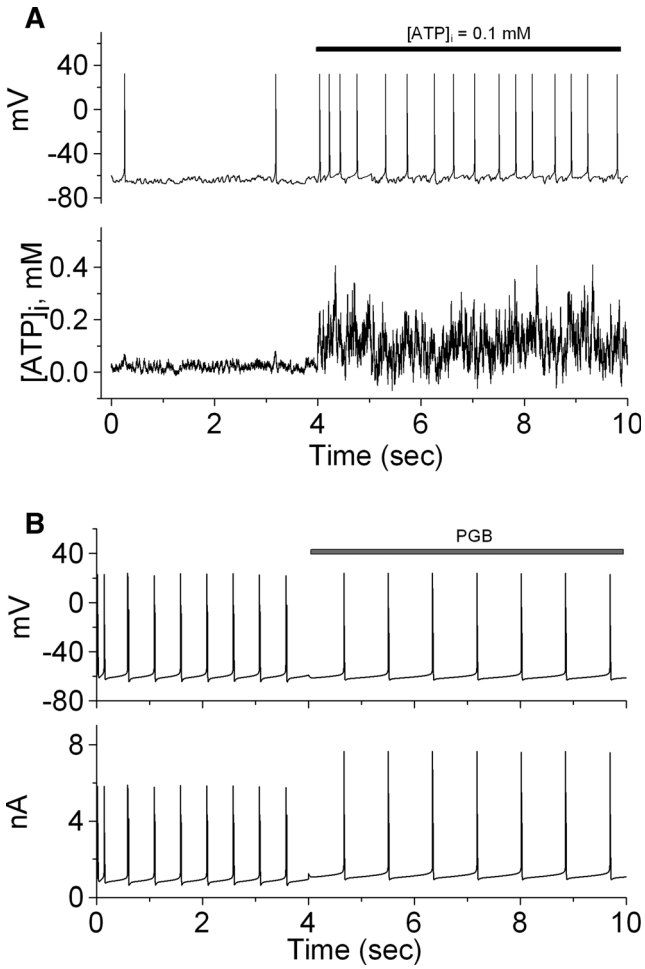


Fig. 6. **A:** Stochastic simulation of intracellular ATP changes on action potential firing. With ATP concentration fluctuation [mean intracellular ATP concentration ($[ATP]_i$) = 0.1 mM; lower panel and bar indicated in upper panel], in addition to depolarization, the firing rate demonstrated irregularity (upper panel). **B:** Maximal probability of channel opening was adjusted to mimic the effects of pregabalin (PGB). PGB (10 μM), indicated as a horizontal bar, was mimicked by an increase in the open probability of $K_{ATP}$ channels, by a factor of 1.3. The firing rate was reduced (upper panel), whereas the amplitude of $K_{ATP}$ currents increased (lower panel).

Furthermore, pregabalin (3-isobutyl GABA; PGB), a novel antiepileptic drug, has been reported recently to be effective in increasing $K_{ATP}$ channel open probability in hippocampal neurons (Huang et al., 2006a). In simulations, maximal probability of channel opening was adjusted to mimic PGB stimulation on $K_{ATP}$ channel activity. As shown in Figure 6B, when maximal probability increased 30%, the firing rate was reduced, along with increased $K_{ATP}$ channel current amplitude. The results show that $K_{ATP}$ channel activity can contribute to the electrical behavior of neurons.

## DISCUSSION

The present study characterizes the properties of $K_{ATP}$ channels in H19-7 neurons. Glucose significantly attenuates $K_{ATP}$ channel activity in a concentration-dependent manner, mainly through a decrease in open probabilities. Additionally, glucose could enhance propagation through inhibition of $K_{ATP}$ channel activity. In simulations, increments of intracellular ATP increase neuronal firing, with ATP fluctuations possibly leading to irregular firing. Moreover, pregabalin, a novel antiepileptic drug, can exert its antiepileptic effect through acting on $K_{ATP}$ channels in this model.

The single-channel conductance, open time (1.71 ± 0.04 msec), channel bursting, ATP sensitivity, and voltage insensitivity observed in these differentiated H19-7 cells were nearly identical to those described for native pancreatic β cells (Kir 6.2/SUR1; Mukai et al., 1998). The H19-7 cell line, as used for studies of development and



ID: kumarpr Date: 22/3/07 Time: 16:47 Path: J:/Production/JNR#/Vol00000/070091/3B2/C2JNR#070091

plasticity in hippocampal neurons, is known to possess the characteristics of hippocampal neurons (Morrione et al., 2000; Bhargava et al., 2002). Despite the heterogeneous expression profiles of $K_{ATP}$ channel subunits reported for hippocampal pyramidal neurons (Zawar et al., 1999), our study emphasized the role of β-cell type $K_{ATP}$ channel in the hippocampus.

Previous studies have shown that lowering glucose levels might prolong the refractory period after excitation, leading to reduced propagation in the central nervous system (Dahlem and Hanke, 2005). The effect of glucose on propagation has been suggested to be related to postsynaptic N-methyl-D-aspartate (NMDA) receptor activities (Abulrob et al., 2005). Our study implies the novel role of $K_{ATP}$ channels. The increment in glucose leads to attenuation of $K_{ATP}$ channel activities, which would enhance field effects of EPSP, potentially caused by electrotonic spread of depolarization, as suggested in our study. Both pre- and postsynaptic $K_{ATP}$ channels were involved in the electrical coupling effects in neurons (Matsumoto et al., 2002). Although postsynaptic $K_{ATP}$ channels interfered with action potential generation and/or presynaptic $K_{ATP}$ channel-limited neurotransmitter release that could contribute to network control (Lee et al., 1997; Liss and Roeper, 2001b), it has been suggested that postsynaptic $K_{ATP}$ channels could be pivotal in neuroprotection and excitability reduction (Yamada and Inagaki, 2005). Our study could support the role of postsynaptic $K_{ATP}$ channel in neuropropagation, in that there were more dominant effects on fEPSP, with a relatively limited effect on presynaptic fiber volley and paired-pulse facilitation in our multielectrode recording system, in the presence of high glucose concentration.

Our simulation also suggested that increments of glucose lead to an increase in firing in hippocampal pyramidal neurons through an inhibitory effect on $K_{ATP}$ channels. It is thus anticipated that openers of β-cell-type $K_{ATP}$ channels, such as diazoxide, might be utilized for selective pharmacological targeting of the $K_{ATP}$ channels in metabolically sensitive neurons sharing the same molecular makeup of Kir6.2 and SUR1 subunits (Liss and Roeper, 2001a) to control seizures that are untreatable by general anticonvulsant drugs (which act on GABA receptors). The simulator model presented here also verified that the new antiepileptic drug pregabalin could decrease neuronal excitability and be antiepileptic by acting on β-cell type $K_{ATP}$ channels in hippocampal neurons (Huang et al., 2006a). Notably, there were also convergent features of the ketogenic diet that may theoretically address $K_{ATP}$ channel activation in how it exerts its antiepileptic effect (Vamecq et al., 2005).

The pathomechanisms remained largely unknown in hyperglycemia-related epileptic seizures. The correlation of blood glucose level and seizure susceptibility has been demonstrated in experimental animal studies (Tutka et al., 1998; Schwechter et al., 2003), but the direct mechanism remains elusive. It has been suggested that $K_{ATP}$ channels play a pivotal role in the persistence of enhanced seizure susceptibility in kindling animals (Jiang et al., 2004). Our study is the first to provide direct evidence that increments of extracellular glucose lead to attenuation of $K_{ATP}$ channel activity in hippocampal neurons; which causes neuronal hyperexcitability, and potentially seizures. The concentration-dependent attenuation of glucose on $K_{ATP}$ channel activity also aids in understanding the higher seizure susceptibility in higher degrees of hyperglycemia (Schwechter et al., 2003). Moreover, the stochastic simulation in this study suggested that, in a state of intracellular ATP fluctuation, which mimics physiological conditions, the neuronal firing pattern would show irregularity. This could be in parallel with the clinical situation in which hyperglycemia-related seizures might develop as a result of paroxysmal action potential development in a steady state of hyperglycemia. From the therapeutic point of view, our study provides a potential role for $K_{ATP}$ channel opening drugs, such as pregabalin, in treating hyperglycemia-related epileptic seizures. Taken together, experimental and simulated findings could account for the seizures associated with the hyperglycemia and hyperglycemia-related neurotoxicity encountered in clinical practice. Our study provides more direct evidence that increments of central neuronal excitability, in a state of high glucose levels, can be attributed to $K_{ATP}$ channel activity attenuation.

## REFERENCES


Abulrob A, Tauskela JS, Mealing G, Brunette E, Faid K, Stanimirovic D. 2005. Protection by cholesterol-extracting cyclodextrins: a role for N-methyl-D-aspartate receptor redistribution. J Neurochem 92:1477–1486.

Ashcroft FM, Gribble FM. 1998. Correlating structure and function in ATP-sensitive $K^+$ channels. Trends Neurosci 21:288–294.

Ashcroft FM, Gribble FM. 2000. New windows on the mechanism of action of $K_{ATP}$ channel openers. Trends Pharmacol Sci 21:439–445. AQ1

Bhargava A, Mathias RS, McCormick JA, Dallman MF, Pearce D. 2002. Glucocorticoids prolong $Ca^{2+}$ transients in hippocampal-derived H19-7 neurons by repressing the plasma membrane $Ca^{2+}$-ATPase-1. Mol Endocrinol 16:1629–1637.

Biessels GJ, Kappelle AC, Bravenboer B, Erkelens DW, Gispen WH. 1994. Cerebral function in diabetes mellitus. Diabetologia 37:643–650.

Dahlem YA, Hanke W. 2005. Intrinsic optical signal of retinal spreading depression: second phase depends on energy metabolism and nitric oxide. Brain Res 1049:15–24.

Dunn-Meynell AA, Rawson NE, Levin BE. 1998. Distribution and phenotype of neurons containing the ATP-sensitive $K^+$ channel in rat brain. Brain Res 814:41–54.

Eaton MJ, Skatchkov SN, Brune A, Biedermann B, Veh RW, Reichenbach A. 2002. SURI and Kir6.1 subunits of $K_{ATP}$ channels are colocalised in retinal glial (Muller) cells. Neuroreport 13:57–60. AQ1

Ermentrout GB. 2002. Simulating, analyzing, and animating dynamical system: a guide to XPPAUT for researchers and students. Philadelphia: Society for Industrial and Applied Mathematics (SIAM).

Eves EM, Tucker MS, Roback JD, Downen M, Rosner MR, Wainer BH. 1992. Immortal rat hippocampal cell lines exhibit neuronal and glial lineages and neurotrophin gene expression. Proc Natl Acad Sci U S A 89:4373–4377.

Gispen WH, Biessels GJ. 2000. Cognition and synaptic plasticity in diabetes mellitus. Trends Neurosci 23:542–549.

AQ1 Gribble FM, Reimann F, Ashfield R, Ashcroft FM. 2000. Nucleotide modulation of pinacidil stimulation of the cloned $K_{ATP}$ channel, Kir6.2/SUR2A. Mol Pharmacol 57:1256–1261.

Griesemer D, Zawar C, Neumcke B. 2002. Cell-type specific depression of neuronal excitability in rat hippocampus by activation of ATP-sensitive potassium channels. Eur Biophys J 31:467–477.

Hernandez-Sanchez C, Basile AS, Fedorova I, Arima H, Stannard B, Fernandez AM, Ito Y, LeRoith D. 2001. Mice transgenically overexpressing sulfonylurea receptor 1 in forebrain resist seizure induction and excitotoxic neuron death. Proc Natl Acad Sci U S A 98:3549–3554.

Hicks GA, Hudson AL, Henderson G. 1994. Localization of high affinity [$^3$H]glibenclamide binding sites within the substantia nigra zona reticulata of the rat brain. Neuroscience 61:285–292.

Higham DJ. 2001. An algorithmic introduction to numerical simulation of stochastic differential equation. SIAM Rev 43:525–546.

Huang CW, Huang CC, Liu YC, Wu SN. 2004. Inhibitory effect of lamotrigine on A-type potassium current in hippocampal neuron-derived H19-7 cells. Epilepsia 45:729–736.

Huang CW, Huang CC, Huang MH, Wu SN, Hsieh YJ. 2005. Sodium cyanate-induced opening of large conductance of calcium-activated potassium channels in hippocampal neuron-derived H19-7 cells. Neurosci Lett 377:110–114.

Huang CW, Huang CC, Wu SN. 2006a. The opening effect of pregabalin on ATP-sensitive potassium channels in differentiated hippocampal neuron-derived H19-7 cells. Epilepsia 47:720–726.

Huang CW, Hsieh YJ, Tsai JJ, Huang CC. 2006b. The effect of lamotrigine on field potentials, propagation and long-term potentiation in rat prefrontal cortex in multi-electrode recording. J Neurosci Res 83:1141–1150.

Jang IS, Nakamura M, Ito Y, Akaike N. 2006. Presynaptic GABAa receptors facilitate spontaneous glutamate release from presynaptic terminals on mechanically dissociated rat CA3 pyramidal neurons. Neuroscience 138:25–35.

Jiang K, Shui Q, Xia Z, Yu Z. 2004. Changes in the gene and protein expression of $K_{ATP}$ channel subunits in the hippocampus of rats subjected to picrotoxin-induced kindling. Brain Res Mol Brain Res 128:83–89.

Kamal A, Biessels GJ, Gispen WH, Ramakers GM. 2006. Synaptic transmission changes in the pyramidal cells of the hippocampus in streptozotocin-induced diabetes mellitus in rats. Brain Res 1073/1074: 276–280.

Kim B, Leventhal PS, Saltiel AR, Feldmann EL. 1997. Insulin-like growth factor-I-mediated neurite outgrowth in vitro requires mitogen-activated protein kinase activation. J Biol Chem 272:21268–21273.

Lee K, Brownhill V, Richardson PJ. 1997. Antidiabetic sulphonylureas stimulate acetylcholine release from striatal cholinergic interneurones through inhibition of $K_{ATP}$ channel activity. J Neurochem 69:1774–1776.

Liss B, Roeper J. 2001a. Molecular physiology of neuronal K-ATP channels. Mol Membr Biol 18:117–127.

Liss B, Roeper J. 2001b. A role for neuronal $K_{ATP}$ channels in metabolic control of the seizure gate. Trends Pharmacol Sci 22:599–601.

Liu M, Seino S, Kirchgessner AL. 1999. Identification and characterization of glucoresponsive neurons in the enteric nervous system. J Neurosci 19:10305–10317.

Margineanu DG, Niespodziany I, Wulfert E. 1998. Hippocampal slices from long-term streptozotocin-injected rats are prone to epileptiform responses. Neurosci Lett 252:183–186.

Matsumoto N, Komiyama S, Akaike N. 2002. Pre- and post-synaptic ATP-sensitive potassium channels during metabolic inhibition of rat hippocampal CA1 neurons. J Physiol 541:511–520.

McCormick DA, Huguenard J. 1992. A model of the electrophysiological properties of thalamocortical relay neurons. J Neurophysiology 68:1384–1400. AQ1

Miki T, Seino S. 2005. Roles of $K_{ATP}$ channels as metabolic sensors in acute metabolic changes. J Mol Cell Cardiol 38:917–925.

Miki T, Liss B, Minami K, Shiuchi T, Saraya A, Kashima Y, Horiuchi M, Ashcroft F, Minokoshi Y, Roeper J, Seino S. 2001. ATP-sensitive $K^+$ channels in the hypothalamus are essential for the maintenance of glucose homeostasis. Nat Neurosci 4:507–512.

Morrione A, Romano G., Navarro M, Reiss K, Valentinis B, Dews M, Eves E, Rosner MR, Baserga R. 2000. Insulin-like growth factor I receptor signaling in differentiation of neuronal H19-7 cells. Cancer Res 60:2263–2272.

Mourre C, Widmann C, Lazdunski M. 1990. Sulfonylurea binding sites associated with ATP-regulated $K^+$ channels in the central nervous system: autoradiographic analysis of their distribution and ontogenesis, and of their localization in mutant mice cerebellum. Brain Res 519:29–43.

Mukai E, Ishida H, Kato S, Tsuura Y, Fujimoto S, Ishida-Takahashi A, Horie M, Tsuda K, Seino Y. 1998. Metabolic inhibition impairs ATP-sensitive $K^+$ channel block by sulfonylurea in pancreatic beta-cells. Am J Physiol 274:E38–E44.

Oka H, Shimono K, Ogawa R, Sugihara H, Taketani M. 1999. A new planar multielectrode array for extracellular recording: application to hippocampal acute slice. J Neurosci Methods 93:61–67.

Okada M, Zhu G, Hirose S, Ito KI, Murakami T, Wakui M, Kaneko S. 2003. Age-dependent modulation of hippocampal excitability by KCNQ channels. Epilepsy Res 53:81–94.

Pinsky PF, Rinzel J. 1994. Intrinsic and network rhythmogenesis in a reduced Traub model for CA3 neurons. J Comput Neurosci 1:39–60.

Pocai A, Lam TK, Gutierrez-Juarez R, Obici S, Schwartz GJ, Bryan J, Aguilar-Bryan L, Rossetti L. 2005. Hypothalamic $K_{ATP}$ channels control hepatic glucose production. Nature 434:1026–1031. AQ1

Quinta-Ferreira ME, Matias CM. 2005. Tetanically released zinc inhibits hippocampal mossy fiber calcium, zinc and synaptic responses. Brain Res 1047:1–9.

Schwechter EM, Veliskova J, Velisek L. 2003. Correlation between extracellular glucose and seizure susceptibility in adult rats. Ann Neurol 53:91–101.

Seino S. 1999. ATP-sensitive potassium channels: a model of heteromultimeric potassium channel/receptor assemblies. Annu Rev Physiol 61:337–362.

Shimono K, Brucher F, Granger R, Lynch G, Taketani M. 2000. Origins and distribution of cholinergically induced beta rhythms in hippocampal slices. J Neurosci 20:8462–8473.

Shoji S. 1992. Glucose regulation of synaptic transmission in the dorsolateral septal nucleus of the rat. Synapse 12:322–332. AQ1

Singh BM, Strobos RJ. 1980. Epilepsia partialis continua associated with nonketotic hyperglycemia: clinical and biochemical profile of 21 patients. Ann Neurol 8:155–160.

Singh BM, Gupta DR, Strobos RJ. 1973. Nonketotic hyperglycemia and epilepsia partialis continua. Arch Neurol 29:187–190.

Stewart R, Liolista D. 1999. Type 2 diabetes mellitus, cognitive impairment and dementia. Diabet Med 16:93–112.

Treherne JM, Ashford ML. 1991. The regional distribution of sulphonylurea binding sites in rat brain. Neuroscience 40:523–531.

Tutka P, Sawiniec J, Kleinrok Z. 1998. Experimental diabetes sensitizes mice to electrical- and bicuculline-induced convulsions. Pol J Pharmacol 50:92–93.

Vamecq J, Vallee L, Lesage F, Gressens P, Stables JP. 2005. Antiepileptic popular ketogenic diet: emerging twists in an ancient story. Prog Neurobiol 75:1–28.

Venna N, Sabin TD. 1981. Tonic focal seizures in nonketotic hyperglycemia of diabetes mellitus. Arch Neurol 38:512–514.

Wu SN, Chang HD. 2006. Diethyl pyrocarbonate, a histidine-modifying agent, directly stimulates activity of ATP-sensitive potassium channels in pituitary GH3 cells. Biochem Pharmacol 71:615–623.

Wu SN, Jan CR, Li HF, Chiang HT. 2000a. Characterization of inhibition by risperidone of the inwardly rectifying $K^+$ current in pituitary GH3 cells. Neuropsychopharmacology 23:676–689.

Wu SN, Li HF, Chiang HT. 2000b. Characterization of ATP-sensitive potassium channels functionally expressed in pituitary GH3 cells. J Membr Biol 178:205–214.

Yamada K, Inagaki N. 2005. Neuroprotection by $K_{ATP}$ channels. J Mol Cell Cardiol 38:945–949.

Yamada K, Ji JJ, Yuan H, Miki T, Sato S, Horimoto N, Shimizu T, Seino S, Inagaki N. 2001. Protective role of ATP-sensitive potassium channels in hypoxia-induced generalized seizure. Science 292:1543–1546.

Yang XJ, Kow LM, Funabashi T, Mobbs CV. 1999. Hypothalamic glucose sensor: similarities to and differences from pancreatic beta-cell mechanisms. Diabetes 48:1763–1772.

Zawar C, Plant TD, Schirra C, Konnerth A, Neumcke B. 1999. Cell-type specific expression of ATP-sensitive potassium channels in the rat hippocampus. J Physiol 514:327–341.

AQ1